International Journal of Chemistry and Material Science Vol. 3(1), pp. 001-011, February, 2015
Available online at http://academeresearchjournals.org/journal/ijcms
ISSN 2327-5553 ©2015 Academe Research Journals

Full Length Research Paper

Study of green and UV emissions in polycrystalline ZnO thin films and spectroscopic properties

Taj Muhammad Khan* and Babar Hussain

National Institute of Lasers and Optronics (NILOP), P.O. Nilore-45650, Islamabad, Pakistan.

Accepted 26 November, 2014

In this paper optical emissions and spectroscopic properties of the polycrystalline ZnO thin film is described. ZnO thin films are produced in oxygen deficit environment and annealed in two different environments with oxygen as common rich element. In oxygen ambient, green emission is quenched and shows no stability, while ultraviolet emission exhibits good stability and enhanced intensity. The green and orange emissions are no longer observed simultaneously, though the orange emission can be obtained at the expense of green emission quenching. Raman spectroscopy demonstrates that intensities of the E2 (high) and E1 (low) modes are strongly dependent on annealing environment. The ratio of E1 (low) modes for the two samples is strongly correlated with the density of oxygen vacancies. Oxygen environment results in smooth morphology and comparatively low roughness. The value of urbach-energy is lower in oxygen ambient compared to those in air. The optical constants (n, k) are calculated using spectroscopic ellipsometry in the wavelength regime of 300–1100 nm. A comparison of energy bandgap, roughness and grain size determined by different techniques is made. These properties have manifested compatibility and promising structural and optical properties of polycrystalline ZnO thin films annealed in oxygen compared to air and can be useful in the fabrication of shorter-wavelength light-emitting devices.

Key words: Nanostructured zinc oxide (ZnO), urbach energy, raman spectroscopy, photoluminescence, thin film, optical properties.

INTRODUCTION

Research background

Zinc oxide (ZnO) is a versatile material used to exhibit various luminescence (PL) bands labeled as near ultraviolet (~UV), yellow-green and near-infrared bands (Zhong et al., 1993; Schirmer and Zwingel, 1970). Compatibility and stability of these luminescence bands are potentially important for different device applications (Takata et al., 1981; Weissenrieder and Muller, 1997). Recently, a considerable attention has been made to this material, because of the UV and yellow-green emissions which are quite appealing for shorter and longer-wavelength devices (Takata et al., 1981; Weissenrieder and Muller, 1997). A prominent feature of this material is the large excitonic binding energy (60 meV), which offers high excitonic emission efficiency above room temperature. Regarding luminescence stability, quenching and possible emission mechanisms in ZnO, research is still in progress to account for the compatibility and research of a conclusive point about this material for various applications. Although many ZnO nanostructures including: thin film, nanoparticles, nanorodes and nanowires, etc. (Weissenrieder and Muller, 1997; Willander et al., 2010) have been synthesized and investigated, ZnO thin film nanomaterial is still under investigation extensively for its remarkable prominent luminescence properties in the UV regime.

*Corresponding author. E-mail: tajakashne@gmail.com. Tel: +92-51-9248671-6; Fax: +92-51-2208051.

For the fabrication of shorter and longer-wavelength optical devices, stability of the luminescence in ZnO material is noteworthy. Photoluminescence from ZnO epilayer on sapphire at room temperature with 325 nm line of He-Cd laser and P-type ZnO:N films prepared by thermal oxidation of Zn_3N_2 have been studied recently (Ding, 2012; Li et al., 2013); however, these reports do not provide a detail study to describe stability and annealing effect on photoluminescence. Similarly, annealing effects for ZnO thin films at different annealing temperatures have also been investigated for different annealing conditions previously (Chu et al., 2003; Shan et al., 2005); however ZnO thin film growth in oxygen deficit environment followed by annealing at higher temperatures without oxygen desorption is rather reported. This work is an extension of the previous studies conducted so far to present a comprehensive detail of luminescence stability and annealing effects in two different ambient conditions (air and oxygen).

Research purposes

In this research work, we present ZnO thin film grown in oxygen deficit environment followed by heat treatment in two different ambient conditions at higher temperatures without oxygen desorption. Luminescence mechanisms, stability of photoluminescence emissions, green luminescence quenching by oxidative annealing, and UV enhancing capability are studied. Spectroscopic study for optical constants (n, k) and morphological analysis for surface quality and subsequent effects on ZnO emissions are also described. Bandgap is determined by different techniques and a comparison is made. Effects of oxygen vacancy density on Raman phonon bands and Urbach energies were also investigated and discussed in detail. On the basis of these results, possible emission mechanisms and light emission modification were considered.

EXPERIMENTAL DETAIL

Nanostructured zinc oxide (ZnO) thin films have been deposited onto fused silica substrates in oxygen deficit environment by e-beam thermal evaporation technique. Before placing substrates in the chamber, they are properly cleaned prior to it with acetone and rinsed in distilled water. The following deposition parameters were used: target (material), ZnO pellet (99.999% pure); substrate, fused silica; substrate temp (Ts), 350°C; substrate to target distance, 35 cm; bam emissions current (I), 20 mA; current (I), 20 A; deposition time, 30 min. The prepared samples were annealed at 1200°C for 1 h in air and oxygen environment.

Diagnostic techniques

X-ray diffraction (XRD) analysis of ZnO thin films was carried out with a Bruker D-8 Discover X-ray diffractometer equipped with a CuKα-radiation (λ=1.54186 Å). Room temperature photoluminescence and Raman spectroscopy measurements were performed with He-Cd laser as an excitation source emitting wavelengths of 442 nm and 325 nm, a triple grating spectrograph (μ-Ramboss MST-4000A, Dongwoo, Optron, Co., Ltd.), equipped with charge coupled device (CCD) and using INDOR software. For photoluminescence, a low transmission cut off filter was used due to unavailability of exact 325 nm cutoff filter.

Surface morphology was investigated by atomic force microscope (AFM) (Quesant Universal SPM, Ambios Technology, USA) (QScope™ 350) in non contact mode. An AFM tip of silicon nitride was used having an approximate radius of curvature of 10 nm.

For transmission measurements, UV-Vis-NIR (Hitachi U-4001) double beam spectrophotometer was used in the spectral range from 250 -1500 nm to assess the film quality for transmission capability.

Spectroscopic ellipsometry (SE) model M2006 VI, J. A. Woollam Co. Inc. 166 consisting of QTH lamp as the light source, and a dual grating scanning monochromator (370–1670 nm) was employed at room temperature in air to measure the optical constants. All the spectra were taken at an angle of incidence of 70° in the desired range from 300-1100 nm. A detail of the experimental diagnostic techniques is also given in our early research reports (Khan et al., 2011). The chemicals used for the deposition of ZnO thin films were of analytical reagent grade (99.99% purity, E-Merck).

RESULTS AND DISCUSSION

Photoluminescence study

Shorter and longer-wavelength light-emitting devices based on ZnO thin films basically ensure emissions stability in this material. Different experimental and theoretical approaches have been proposed to understand the phenomena of emissions stability and the mechanisms responsible for these emissions (Lin et al., 2001; Hsieh et al., 2007; Kuo et al., 2006; Ye et al., 2005).

Figure 1 shows that PL spectrum of ZnO thin film has taken in the wavelength range of our interest from 200-800 nm using 325 nm as the excitation wavelength. It is noteworthy to mention here that ZnO exhibits different luminescence bands which are labeled as, near ultraviolet (~UV), green-yellow and orange bands respectively (Umar et al., 2009). For the sample annealed in the air at 1200°C, UV and green emissions are observed at 372 and 538 nm (Figure 1), while no yellow-orange emission can be seen. However, for the sample annealed in oxygen ambient at 1200°C, the subsequent emissions are observed at 368 and 544 nm together with

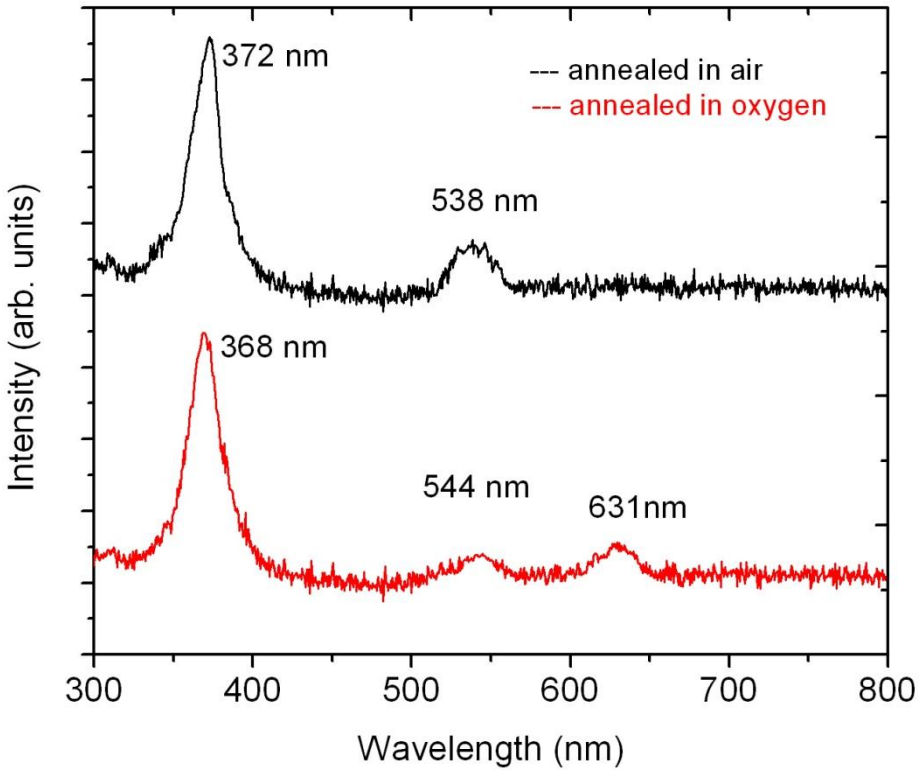

Figure 1. Room temperature photoluminescence spectrum of ZnO thin films annealed in air and oxygen environment.

a yellow-orange emission which is peaked at 630 nm. These emissions are well similar with previous theoretical and experimental reports (Ding, 2012; Nanto et al., 1981; Shan et al., 2007). The orange emission in the range from 610 - 630 nm can be related to oxygen interstitials (Oi) (Xu et al., 2009). From Figure 1, it can be seen that UV and green emissions are blue and red-shifted respectively. It could be concluded that the samples after post annealing in air and oxygen exhibit very different dominant emissions in the ultraviolet (UV), yellow-green and yellow-orange regions. For the oxygen annealing environment, green emission diminishes while yellow-orange emission appears prominently. However, when sample is annealed in the air environment, it shows almost similar behavior as observed for the sample heat treated in the oxygen environment. Green emission is mainly associated with oxygen vacancies. For the green emission, diminishing intensity is explained as: the absorbed oxygen molecules on the surface of the film are gradually penetrating into the film to fill the oxygen vacancies near the surface and consequently the emission intensity which is falling down (Lin et al., 2001). Nevertheless, in our case, the most intense UV and green–yellow emissions are observed from oxygen deficit sample (annealed in air). The initial enhanced intensity for green emission (air annealing) is gradually quenched after annealing in oxygen. This green emission is mainly associated with the density of oxygen vacancies and has been explained by different researchers (Tay et al., 2010; Linhua et al., 2009). In fact due to annealing in oxygen environment, many oxygen atoms which are absorbed on the surface of the film reduce density of oxygen vacancies and results in the suppression of green emission. It has be shown that by further increasing the annealing temperature, green emission reappears because annealing at higher temperature may cause the enhancement of green emission due to desorption of oxygen atoms that start to occur from the surface of the film and generate more oxygen vacancies.

Regarding luminescence in ZnO thin film, it has been reported that with increase of aging time, green emission gradually decreases while ultraviolet emission either increases or shows no significant change. The reason for this phenomenon is more likely the gradually filling-up of the mechanism of oxygen vacancies in ZnO (Linhua et al., 2009). Both green and orange emissions can be related to the amount of oxygen in the film. The green luminescence comes from oxygen deficient sample while the orange emission comes from oxygen rich film. This conclusion pertains to the importance of the role played

by oxygen in ZnO emissions. Figure 1 illustrates that strong yellow-green and orange emission cannot be observed simultaneously and orange emission is obtained only at the expense of green emission quenching. Dispute related to the green emission that has been proposed by different researchers in their reported work is mainly connected with the oxygen related defects such as, oxygen interstitial and oxygen antisites; and its emission mechanism is established by the oxygen vacancies. Energy bandgap is determined from the PL data which are 3.34 and 3.37 eV for the sample annealed in air and oxygen respectively. The blue-shift in UV-emission, which is the so-called band-gap emission for the film annealed in oxygen ambient, can be associated to compressive strain (C_{zz} = $(C - C_0)/C_0$), where C is the lattice parameter of the strained ZnO film and C_0 is the unstrained lattice parameter of ZnO along the *c*-axis. The above mentioned strain is also associated with the bandgap (Eg) of the material. An increase in the bandgap determined by PL is better explained using strain and bandgap relationship. According to this relation, $E_g = A - BC_{zz,}$ where C_{zz} is the strain along c-axis is determined by the aforesaid formula. Now for a compressive strain ($C_{zz,}$), the second term becomes positive and the E_g value increases. This reflects that for the developed compressive strain in the sample, the corresponding bandgap is increased. This feature can also be observed in the Raman spectrum of ZnO thin film where up-shift of E_2 (high) mode is associated with the compressive strain in the film.

For determining crystallite size, peak wavelength of the UV emission is used in the equation based on effective mass approximation given by Brus. This equation is derived using effective mass model which describes particle size D=2r (r, radius) as a function of peak emission wavelength (λ_p nm). The crystallite size determined are about 64 and 57 nm for the samples annealed in air and oxygen respectively. These results are closely matched with the AFM analysis which will be discussed subsequently. To further signify our results, we have correlated crystallite size and energy bandgap (blue-shift) by effective-mass approximation. Based on this approximation, size dependence of band gap (E*) can be represented as follows:

$$E^* = E_g + \frac{h^2}{8\,\mu R^2} - \frac{1.8e^2}{4\pi\epsilon_0\epsilon_\alpha R} \quad \text{..... (1)}$$

Where E_g is the bandgap of the material, μ is the effective mass of the exciton given by ($\mu = 1/m^*_e + 1/m^*_h$), ϵ_o is the permittivity of the material and ϵ_α is the high-frequency dielectric constant.

Equation 2 provides an obvious manifestation of the increase in band gap with particle size. For absolute values of the shift in band edge as a function of particle size (R), the conduction electrons (e) and valence holes (h) bands can be given by the following expressions:

$$(e) = E_g + \frac{h^2}{8\,m_e^* R^2} - \frac{0.9e^2}{4\pi\epsilon_0\epsilon_\alpha R} \quad \text{..... (2)}$$

$$(h) = E_g + \frac{h^2}{8\,m_h^* R^2} - \frac{0.9e^2}{4\pi\epsilon_0\epsilon_\alpha R} \quad \text{..... ..... (3)}$$

where m_e* is the effective-mass of electron and m_h* is the effective-mass of hole, and for ZnO, the effective masses of electrons and holes are $0.24m_0$ and $0.45m_0$, respectively.

Now from the above mentioned formula, if we assume that the position of the energetic UV emission of the deeply trapped charge carrier is independent of the crystallite size, shift of the energetic position of trapped emission as a function of particle size can be determined by the shift of conduction- or valence-band edge. Furthermore, as a consequence, mechanisms responsible for the luminescence in ZnO can be established with the help of these approximations.

From the above results, it is established that ultraviolet emission in ZnO thin film is caused by band to band transition of electron from conduction band to valance band. This emission is practically stable while green emission due to oxygen vacancies is incompatibly unstable. This furnishes the idea of its unsuitability for longer-wavelength light-emitting devices. Similarly, orange emission due to oxygen interstitials can be obtained at the expense of green emission. Therefore, under common conditions, ZnO material is suitable for the fabrication of ultraviolet light emitting (LED) devices.

Raman spectroscopy analysis

The typical Raman spectrum of the samples taken with He-Cd laser source (excitation wavelength 442 nm) is shown in Figure 2. In this spectrum, the observed phonon frequencies are: E_2 (high) - E_2 (low) 328 cm^{-1}, E_2 (high) 430-436 cm^{-1}, E_1 (LO) 578 cm^{-1} and (2LO) 1146 cm^{-1}. The various phonon modes indicate that in polycrystalline ZnO thin film, molecular dipole moments oscillate along different crystal directions. E_1 (LO) has often been reported at the frequency range from (570-590) cm^{-1} and is interpreted as an indication of oxygen deficiency in ZnO thin films (Alim et al., 2005; Yahia et al., 2008). The phonon mode located at 578 cm^{-1} is the longitudinal optical (LO) phonon mode of ZnO with E_1 symmetry and it clearly reflects the presence of defects (like defects attributed due to oxygen vacancies and Zn interstitials). For film annealed in air, this mode is prominent because of oxygen deficiency. However, for the film annealed in oxygen ambient, it shows diminishing behavior. The E_2

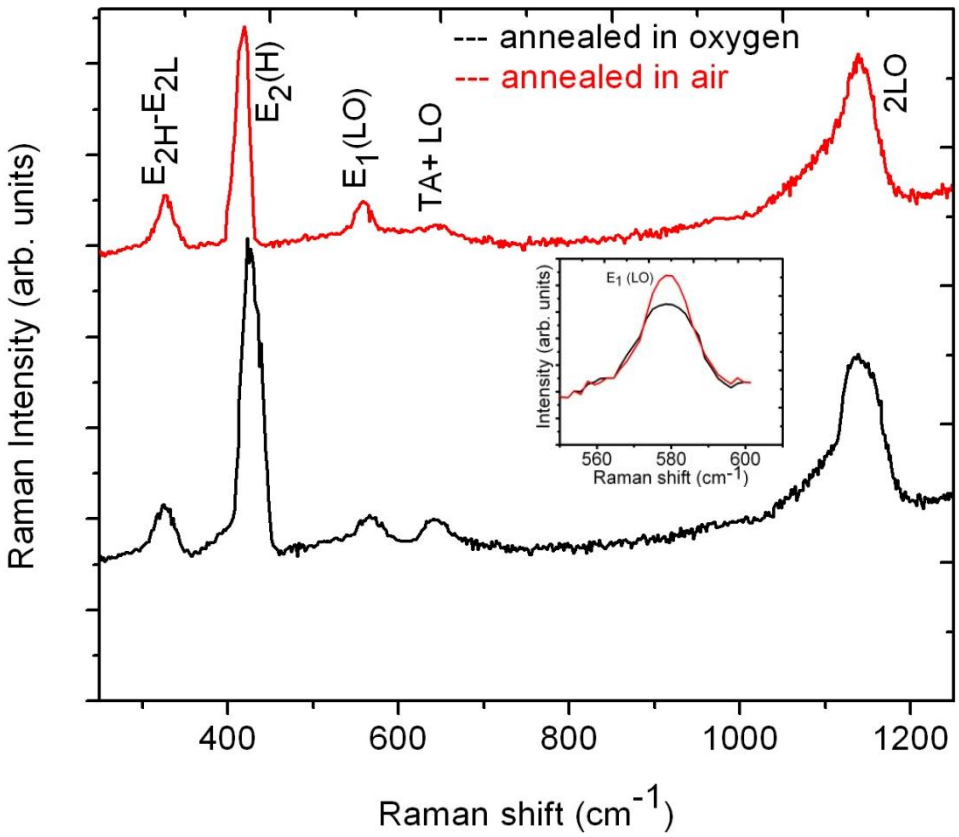

Figure 2. Room temperature of Raman spectrum of ZnO thin films annealed in air and oxygen ambient (inset shows intensity ratio of E_1 (LO) phonon modes for the two samples).

mode is non-polar but consists of E_2 (low) and E_2 (high) frequency modes, characteristic of the wurtzite structure ZnO (Yahia et al., 2008). The mode at wave number 328 cm^{-1} encompasses the second order Raman scattering from the E_2 (high) - E_2 (low) multiple scattering processes. The strong line lies at 430-436 cm^{-1} corresponding to E_2 (high) mode of ZnO and is the band characteristic of wurtzite-structure ZnO. Raman intensity of this peak is inter-connected to the crystalline structure, quality of the film and density of oxygen vacancies. The peak at 1146 cm^{-1} cannot be explained within the framework of single phonon modes and is attributed to multiple phonon scattering processes (2LO) (Alim et al., 2005).

The intensity and shift of the E_2 (high) phonon frequency gives considerable information on stress and strain analysis of the film. Previous investigations showed a relation between stress and the E_2 (high) mode frequency; under a compressive stress, E_2 (high) mode leads to a upshift, whereas a tensile stress leads to a downshift of the E_2 (high) mode (Harriman et al., 2013). The upshift in the E_2 (high) mode for the film annealed in oxygen compared to film annealed in air reflects that compressive strain is produced in the deposited thin film after annealing in oxygen. This is well accorded to the increase in the optical bandgap as determined by PL according to the relation mentioned in the PL description, that is, $E_g = A - BC_{zz,}$ where C_{zz} is the strain along c-axis. Hence our PL results are well in agreement with Raman analysis. The increased Raman intensity for the sample annealed in oxygen indicates a high quality crystalline thin film with good stiochiometry ratio. In contrast, to the case of annealing in air, mode E_1 (LO) became intense as demonstrated in Figure 2 (inset). The peak at 578 cm^{-1} corresponds to E_1 (LO) mode of ZnO and is related to oxygen vacancies and zinc interstitials (Zhang, 2006). For the annealed sample in oxygen, the peak intensity of E_1 (LO) mode obviously declines, because oxygen defects density in the film is dropped. By considering the dipole changes induced by oxygen vacancies and derivation based on density functional theory, an oxygen vacancy density is shown to be responsible for the frequency shift and broadening of the Raman active phonon mode. Comparison of the Raman spectrum of oxygen deficit and stiochiometry thin film demonstrates the importance of other factors such as polar grain boundaries in the lattice dynamical behavior of thin films.

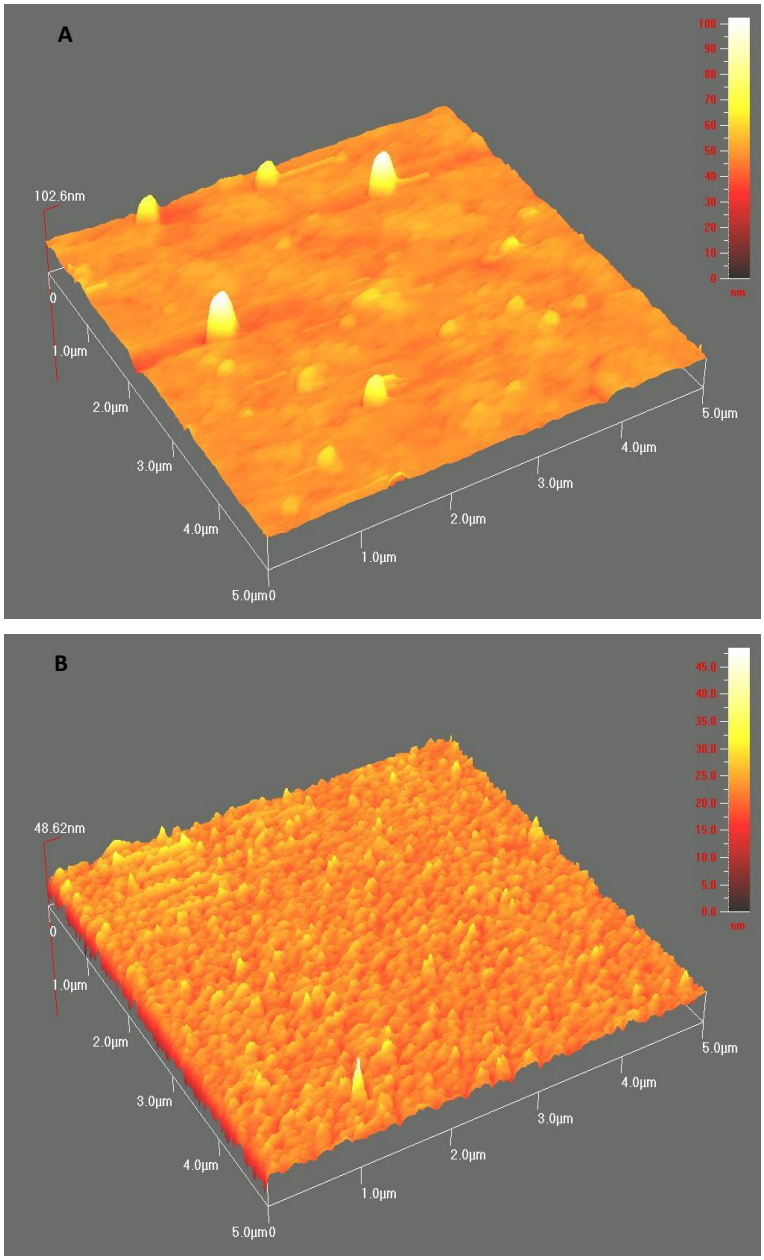

Figure 3. AFM 3-D images (in tapping mode) of ZnO thin films annealed in air and oxygen for the same annealing time.

Moreover, broadening of E_2 (high) phonon mode is due to decrease in grain size. The ratio of intensities of E_1 (LO) in air to E_1 (LO) in oxygen is shown by the inset in Figure 2. Therefore, it is suggested that green emission is mainly connected with oxygen vacancies.

Atomic force microscopy analysis

Surface morphology was examined by employing Atomic Force Microscopy (AFM) in the non-contact mode. AFM 3-D images of ZnO thin films are shown in Figure 3. Both films show best ordering, smoothness and compact morphology (Figure 3a, b). Apparently, the films have good adhesion with substrates, and its surface presents a low roughness value which suggests formation of smooth and compact ZnO thin film after annealing. However, after annealing in air, film surface is rough (Figure 3a) compared to film annealed in oxygen environment. The

Table 1. A comparison of the calculated/measured values by different techniques for ZnO thin films.

	Annealed in air				Annealed in oxygen			
Technique employed	**Band-gap (eV)**	**Thickness (nm)**	**Roughness (nm)**	**Grain size (nm)**	**Band-gap (eV)**	**Thickness (nm)**	**Roughness (nm)**	**Grain size (nm)**
SE	3.32	147	13	---	3.45	139	21	---
PL	3.34	---	---	64	3.37	---	---	57
AFM	---	131	11	52	---	127	7	47
PS	3.35	---	--	---	3.49	---	--	---

data associated with root mean-square (rms) roughness, and grain size of the film is measured by the software attached with AFM machine and the linear intercept method respectively. Resultantly, data of the foresaid quantities (rms roughness, and grain size) is summarized in Table 1.

Phtospectrometry study

For the optical analysis, double beam phtospectrometry measurements were performed. Transmittance (T) is taken in the spectral range of our interest from 250 and 2500 nm. The behavior of transmission spectra is oscillatory because of thin film interference (Figure 4a). The transmittance spectrum for annealed ample in oxygen reveals a high transmission of 89.9% in the near infrared region (≤900 nm) which decreases and remains more or less constant to about less than 80% in the higher wavelength region. Due to annealing in the oxygen atmosphere, more oxygen rush to be absorbed on the film surface to fill the vacancies and reduce the grain boundaries account for the transmission loss. The maximum transmission of 73.5% is observed at (≤900 nm) for the sample annealed in air and reduces to 62.4% in the higher wavelength regions. Nevertheless, transmittance slowly decreases through the IR region. It is evident that both films have uniform transmittance in the higher wavelength (IR) region. It can be explicated that thin films deposited in oxygen deficit environment and annealed in the air lack oxygen atoms with low optical transmittance and yellow coloration. On the other hand, in the case of excessive oxygen atoms existing in the film, interstitial or grain boundary oxygen atoms trap free electrons which absorb radiation in the infrared region, thereby causing reduction in the transmission (Leeuwen et al., 1995).

Transmission spectrum is used to calculate bandgap for both samples using the relation between thin film absorption coefficient (α) and the photon energy ($h\upsilon$) for direct allowed transition (Collins, 2005):

$$(\alpha h\upsilon)^2 = A(h\upsilon - E_g) \quad \text{..... (4)}$$

Where α is the absorption coefficient ($\alpha=4\pi K/\lambda$), $h\upsilon$ is the photon energy, E_g is the band gap and A is constant with separate values for different transitions. We extrapolated the linear part of the curve $(\alpha h\upsilon)^2$ Vs ($h\upsilon$) to the energy axes to obtain E_g as shown in Figure 4b. The energy gap (E_g) so obtained is 3.35 eV for the sample annealed in air and 3.49 eV for the film annealed in oxygen and closely agree with the values reported elsewhere for the polycrystalline ZnO thin films (Asmar et al., 2005). The low E_g value for the sample annealed in air is due to oxygen deficiency in the sample because of the excess zinc produced during the growth which occupies the interstitial positions in the crystal lattice and formed as native defects.

At the grain boundaries, the assembled Zn metals act as large body barrier to scatter light instead of to transmit it, hence the oxygen deficit sample presents a low transmission and low value of energy gap (E_g). The energy band-gaps values calculated by phtospectrometry are closely matched with the values obtained from the PL and ellipsometry measurements. Another important parameter calculated for both samples is the Urbach energy.

For Urbach energy (E_u), it is assumed that the absorption coefficient (α) near the band edge shows an exponential dependence on photon energy for many materials and this dependence is given by Collins, 2005:

$$\alpha = \alpha_o \exp\left(\frac{h\upsilon}{E_u}\right) \quad \text{..... (5)}$$

Where α_o is a constant and E_u is the Urbach energy which is the width of the tails of the localized state associated with the amorphous state in the forbidden band. From the plot of lnα versus photon energy (hυ) plots for oxygen deficit and annealed ZnO thin films (not shown), the values of Urbach energy at the band edge, ~3.35 eV and ~3.49 eV, are obtained as 102.4 meV and 92.3 meV for the samples annealed in air and oxygen respectively. The decrease in Urbach energy can be attributed to a decrease in thermal induced structural disorder and improved crystalline structure for the sample annealed in oxygen environment.

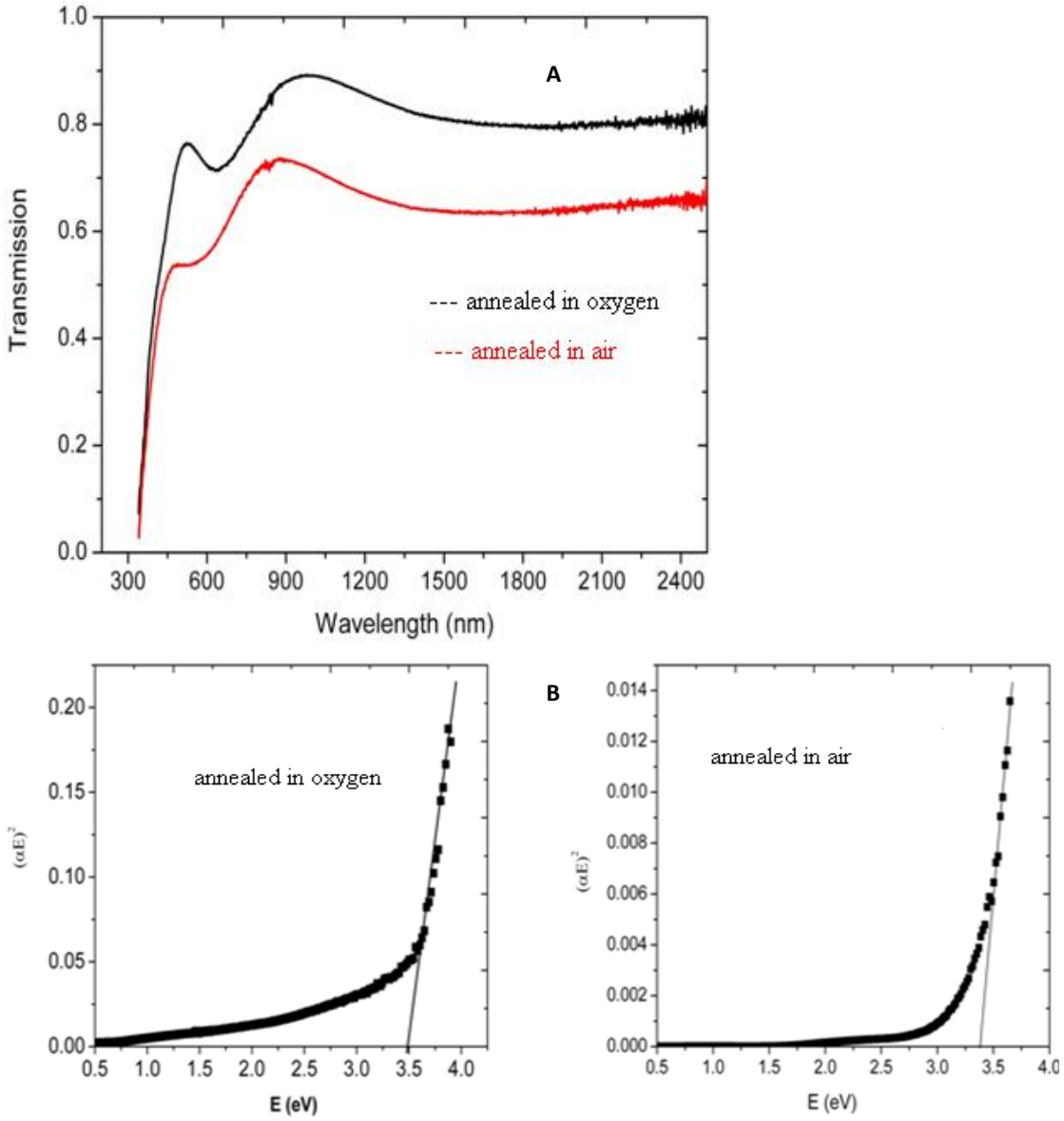

Figure 4. (A) Transmission spectrum of ZnO thin films annealed in air and oxygen environment in the wavelength regimes from 250 and 2500 nm. (B) Band-gap calculation of ZnO thin films annealed in air and oxygen environment.

Spectroscopic ellipsometry (SE) analysis

The ellipsometry measurements are performed with SE using XE lamp. These measurements allow us to determine the dispersion law of the complex refractive index (ñ = n - jk). The optical constants like, refractive index (n), extinction coefficient (k) and dielectric constants (e) were simulated using Cauchy multilayer model (Bond, 1965). Thickness, roughness and band-gaps of the films were determined and compared with the values obtained by other techniques. The Cauchy dispersion relations for this model are given by the following equations (Bond, 1965):

$$n(\lambda) = A_n + \frac{B_n}{\lambda^2} + \frac{C_n}{\lambda^4} \quad \text{(6a)}$$

$$k(\lambda) = k_0 + \frac{C_0 k_1}{\lambda^2} + \frac{C_1 k_2}{\lambda^4} + \quad \text{(6b)}$$

$$k = k_{amp} \cdot e^{\exp(E - Bandedge)} \quad \text{(6c)}$$

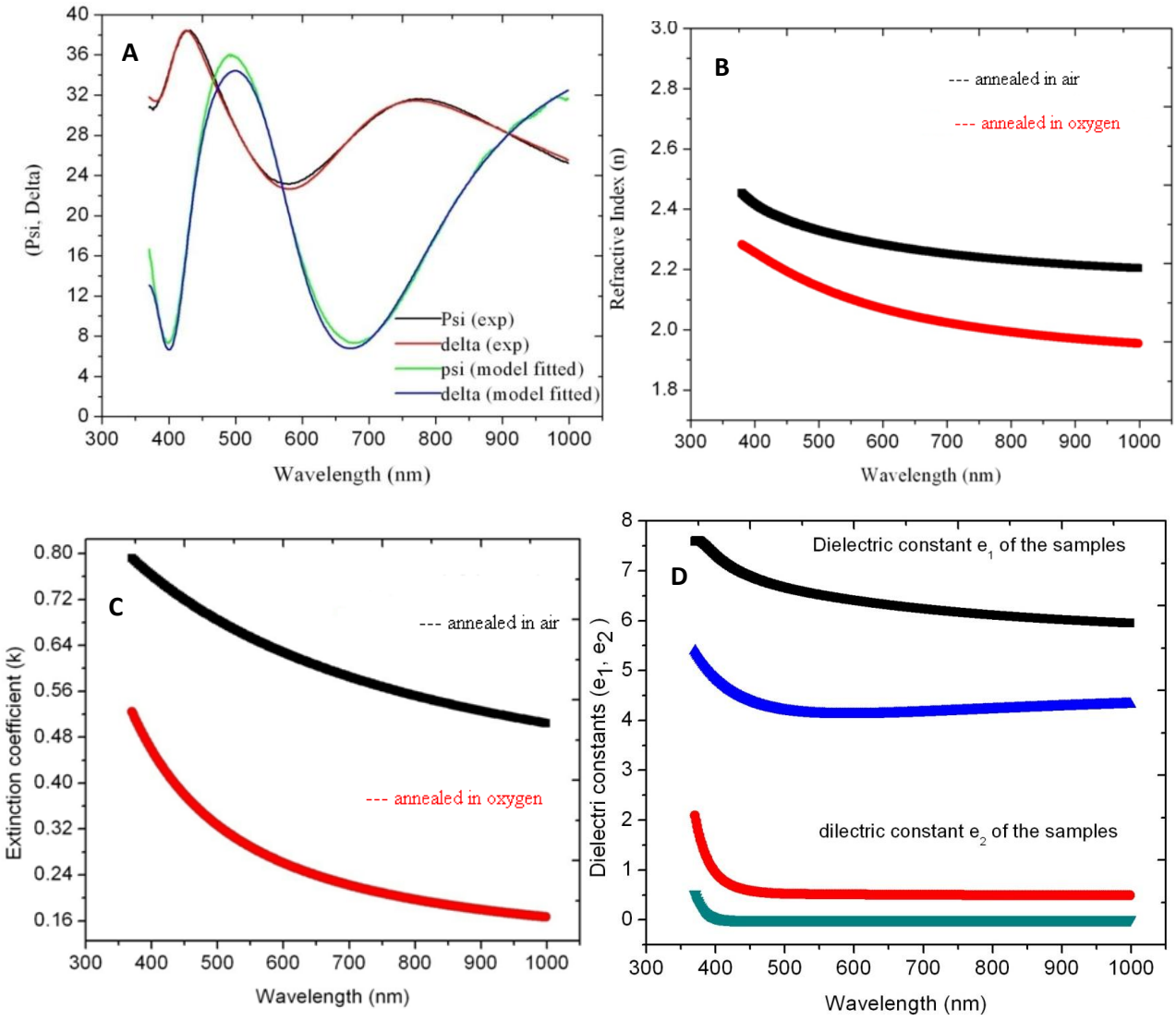

Figure 5. (A) Psi and Delta curve fitting of experimental and theoretical data using Cauchy model. (B) Spectrum of refractive index versus wave length of ZnO thin films annealed in air and oxygen environment. (C) Spectrum of extinction coefficient versus wave length of ZnO thin films annealed in air and oxygen environment. (D) Spectrum of dielectric constants versus wavelength of ZnO thin films annealed in air and oxygen environment.

The A, B, C parameters are variable fit parameters that determine the index dispersion. The *k* amplitude and exponent are fit parameters for determining the shape of the extinction coefficient dispersion.

Psi (ψ) and delta (Δ) spectra were measured at the incidence angle of 70° over the range: Psi (ψ) = 0° – 350 90°, delta (Δ) = 0° – 360° in the spectral wavelength range of 300 - 1100 nm. Calculated ψ and Δ spectra were analyzed by fitting with the theoretical values through simulation and best fitting parameters n_0 = 1.909, n1 = -406.9, n_2 = 664.2, k_0 = 0.234, k_1 = 74.87 and k_2 = 765.615. Calculated and simulated ψ and Δ spectra are shown in Figure 5a. The experimental values are well satisfied with the simulated values obtained by curve fitting. Observed and simulated values based on the Cauchy Model are much closed to each other and is manifested in that the model used was exact. The low value of MSE error is 0.6587 also indicating the exactness of the model. On the basis of this fitting, other optical constants refractive index (n) and extinction coefficient (k) were simulated. The resulting refractive index spectral dispersion is in good agreement with the reported data in the literature (Dumont et al., 1999). The real refractive index (n), extinction coefficient (k) and

dielectric constants (e_1, e_2), as a function of wavelength for ZnO thin film samples annealed in air and oxygen are shown in Figure 5b, c, d. We observe a clear difference in refractive index (n) and extinction coefficient (k) for the samples: in particular, n is higher for the sample annealed in air (2.44-2.20) and lower for the sample annealed in oxygen (2.27-1.97). The refractive index and extinction coefficient exhibits almost linear variation from ultraviolet (UV) to near infrared (IR). The variation between the refractive indices and k values of the films grown in oxygen deficit environment and annealed in air and oxygen can be explained assuming that oxygen atoms exceeding the stoichiometry are interstitial between the lattice planes, thereby influencing the optical properties. Thus, the possibility to control the refractive index by the oxygen deficit environment during the deposition can be usefully exploited for the optoelectronic applications. It would be possible to use this phenomenon to realize a dielectric structure with tailored refractive index profile in order to confine electromagnetic radiation and take advantage of the piezoelectric properties of ZnO. Moreover, the bandgap energies determined by a linear fit of the transmittance spectrum are about 3.32 and 3.45 eV for the samples annealed in air and oxygen environment respectively. For the samples annealed in air and oxygen, the average film thicknesses obtained by cure fitting using Cauchy layer model were about 147 and 139 nm, while the average roughness was found to be 21 and 13 nm respectively. The values so obtained by SE technique are well in agreement with those obtained by phtospectrometry, PL and AFM.

CONCLUSION AND OUTLOOK

The effect of annealing ambient (air, oxygen) on the structural and particularly optical luminescence properties of polycrystalline ZnO thin films are investigated in oxygen deficit environment. Oxygen plays a very significant role in the luminescence of ZnO thin films. The green emission due to oxygen vacancies diminishes due to oxidative annealing. The strong yellow-green and orange emissions cannot be observed simultaneously. On the basis of fundamental luminescence stability, ZnO thin films are suitable for the fabrication of ultraviolet light emitting devices and unsuitable for the fabrication of green light emitting devices. The intensity and upshift of E_2 (high) and E_1 (low) phonon modes are strongly correlated with the density of oxygen vacancies and compressive strain in the films. The deposited films after annealing in oxygen environment have smooth surface compared to the film annealed in air. Low transmission and low optical bandgap is observed for the sample annealed in air and reflects oxygen deficit thin film. The Urbach energy is 102.4 and 92.3 meV for the sample annealed in air and oxygen atmosphere respectively. Spectroscopic ellipsometry shows the possibility of controlling refractive index through oxygen deficit ambient during deposition of thin film and can be usefully exploited for optoelectronic applications. It will be possible to use this phenomenon to realize a dielectric structure with tailored refractive index profile in order to confine electromagnetic radiation and take advantage of the piezoelectric properties of ZnO thin film.

ACKNOWLEDGEMENTS

The authors wish to thank their parent department, NILOP, Photonic division Islamabad, particularly nano-devices group for providing the required facilities for this research work. They also acknowledge PIEAS University Islamabad for providing AFM facility and M. Nasir for providing optical filter for photoluminescence measurements.

REFERENCES

Alim KA, Fonoberov VA, Shamsa M, Balandin AA (2005). Micro-raman investigation of optical phonons in ZnO nanocrystals. J. Appl. Phys. 97: 124313-124313-5.

Asmar RA, Ferblantier G, Sauvajol JL, Giani A, Khoury A, Foucaran A (2005). Fabrication and characterization of high quality zno thin films by reactive electron beam evaporation technique. J. Microelectr., 36: 694-699.

Bond WL (1965). Measurement of the refractive indices of several crystals. J. Appl. Phys., 36: 1674-1681.

Chu SY, Water W, Liaw JT (2003). Influence of post deposition annealing on the properties of ZnO films prepared by Rf magnetron sputtering technique. J. Eur. Ceram. Soc. 23: 1593-1598.

Collins RW, Ferlauto AS In Handbook Of Ellipsometry Edited By Tompkins HG And Irene EA (2005). (Norwich New York: William Andrew) pp. 125–129

Ding BF (2012). Chin. zno thin film deposition on sapphire substrates by chemical vapor deposition. Phys. Lett. 29: 03820-038205.

Dumont E, Dugnoille B, Bienfait S (1999). Simultaneous Determination Of The Optical Properties And Of The Structure Of R.F.-Sputtered Zno Thin Films. Thin solid films 353: 93-99.

Harriman TA, Bi Z, Jia QX, Lucca DA (2013). Frequency shifts of the e_2 high raman mode due to residual stress in epitaxial zno thin films. J. Appl. Phys. Lett., 103: 121904-121904-4.

Hsieh PT, Chen YC, Kao KS, Lee MS, Cheng CC (2007). The ultraviolet emission mechanism of zno thin film fabricated by sol-gel technology. J. Eur. Ceram. Soc., 27: 3815-3818.

Khan TM, Mehmood MF, Mahmood A, Shah A, Raza Q, Iqbal A (2011). Synthesis of thermally evaporated znse thin film at room temperature. Thin Solid Films, 519: 5971-5977.

Kuo SY, Chen WC, Cheng CP (2006). investigation of annealing-treatment on the optical and electrical of properties of sol–gel-derived zinc oxide thin films. Superlat. Microstruct., 39: 162-170.

Leeuwen Ra, Hung CJ, Kammler DR, Swizer JA (1995). Optical and electronic transport properties of electrodeposited thallium (iii) oxide films," J. Phys. Chem J. Phys. Chem., 99: 15247-15252.

Li M, Wang JZ, Zhang BS, Li Q (2013). P-type ZnO:N films prepared by thermal oxidation of Zn_3N_2. Chin. Phys. Lett., 30(2): 027303-027306.

Lin B, Fu Z, Jia Y (2001). Green luminescent center in undoped zinc oxide films deposited on silicon substrates. Appl. Phys. Lett., 79: 943-945.

Lin B, Fu Z, Jia Y (2001). Green luminescent center in undoped zinc oxide films deposited on silicon substrates. Appl. Phys. Lett., 79: 943-945.

Linhua X, Linxing S, Xiangyin L (2009). Preparation of nanocone zno thin film and its aging effect of photoluminescence. J. App. Surf. Sci., 255(11): 5957-5960

Nanto H, Minami T, Takata S (1981). Photoluminescence in sputtered zno thin films phys. status solidi a 65: k131-k134.

Schirmer OF, Zwingel D (1970). The Yellow Luminescence Of Zinc Oxide. Solid State Commun., 8: 1559-1563.

Shan FK, Liu GX, Lee WJ, Shin BC (2007). the role of oxygen vacancies in epitaxial-deposited ZnO thin films. J. Appl. Phys., 101: 053106-053108.

Shan FK, Liu GX, Lee WJ, Lee GH, Kim IS, Shin BC, Kim YC (2005). Transparent conducive zno thin films on glass substrates deposited by pulsed laser deposition. J. Cryst. Growth, 277: 284-292.

Takata S, Minami T, Nanto H, Kawamura T (1981). Temperature dependence of electro- and photoluminescence in zno single crystals. phys. status solidi a 65: k83-k86.

Tay YY, Tan TT, Boey F, Liang Mh, Ye J, Zhao Y, Norby T, Li S (2010). Correlation between the characteristic green emissions and specific defects of zno. J. Phys. Chem. Chem. Phys., 12: 2373-2379.

Umar A, Ribeiro C, Hajry AA, Masuda Y, Hahn YB (2009). Growth of highly c-axis-oriented zno nanorods on zno/glass substrate: growth mechanism, structural, and optical properties. J. Phys. Chem., 113: 14715-14720.

Weissenrieder KS, Muller J (1997). Conductivity model for sputtered zno- thin film gas sensors. Thin Solid Films, 300: 30-41.

Willander M, Nur O, Sadaf JR, Qadir MI, Zaman S, Zainelabdin A, Bano N, Hussain I (2010). Luminescence from Zinc Oxide Nanostructures and Polymers and Their Hybrid Devices. J. Mat., 3(4): 2643-2667.

Xu L, Shi L, Li X (2009). Preparation Of Nanocone Zno Thin Film And Its Aging Effect Of Photoluminescence. J. App. Surf. Sci., 255: 5957-5960.

Yahia S, Znaidi L, Kanaev A, Petitet J (2008). Raman study of oriented zno thin films deposited by sol-gel method. spectrochim. Acta. Mol. Biomol. Spectrosc., 71(4): 1234-1238.

Ye JD, Gu SL, Qin F, Zhu SM, Liu SM, Zhou X, Liu W, Hu LQ, Zhang R, Shi Y, Zheng YD (2005). Correlation between green luminescence and morphology evolution of zno films. Appl. Phys., A 81: 759-752.

Zhang Y (2006). Micro-raman studies of li doped and undoped zno needle crystals. J. Phys. Condens, Matter., 18: 957-963.

Zhong J, Kitai AH, Mascher P, Puff W (1993). The influence of processing conditions on point defects and luminescence centers in ZnO. Electrochem. Soc., 140: 3644-3649.